Pharm Res (2011) 28:2575–2588
DOI 10.1007/s11095-011-0485-7

RESEARCH PAPER

Potential of Amino Acid/Dipeptide Monoester Prodrugs of Floxuridine in Facilitating Enhanced Delivery of Active Drug to Interior Sites of Tumors: A Two-Tier Monolayer *In Vitro* Study

Yasuhiro Tsume • John M. Hilfinger • Gordon L. Amidon

Received: 1 November 2010 / Accepted: 16 May 2011 / Published online: 14 June 2011

ABSTRACT

Purpose To evaluate the advantages of amino acid/dipeptide monoester prodrugs for cancer treatments by assessing the uptake and cytotoxic effects of floxuridine prodrugs in a secondary cancer cell monolayer following permeation across a primary cancer cell monolayer.

Methods The first Capan-2 monolayer was grown on membrane transwell inserts; the second monolayer was grown at the bottom of a plate. The permeation of floxuridine and its prodrugs across the first monolayer and the uptake and cell proliferation assay on secondary layer were sequentially determined.

Results All floxuridine prodrugs exhibited greater permeation across the first Capan-2 monolayer than the parent drug. The correlation between uptake and growth inhibition in the second monolayer with intact prodrug permeating the first monolayer suggests that permeability and enzymatic stability are essential for sustained action of prodrugs in deeper layers of tumors. The correlation of uptake and growth inhibition were vastly superior for dipeptide prodrugs to those obtained with mono amino acid prodrugs.

Conclusions Although a tentative general overall correlation between intact prodrug and uptake or cytotoxic action was obtained, it appears that a mixture of floxuridine prodrugs with varying beneficial characteristics may be more effective in treating tumors.

Y. Tsume • G. L. Amidon (✉)
Department of Pharmaceutical Science, University of Michigan
Ann Arbor, Michigan 48109, USA
e-mail: glamidon@umich.edu

J. M. Hilfinger
TSRL, Inc.
Ann Arbor, Michigan 48108, USA

KEY WORDS antiproliferative action · Capan-2 pancreatic cancer cells · *in vitro* tumor model · mono amino acid and dipeptide monoester floxuridine prodrugs · permeation and bioactivation · prodrug cocktail · two-tier Capan-2 monolayer · two-tier Capan-2 pancreatic cancer monolayer

INTRODUCTION

Chemotherapy has been widely used for various cancer treatments. However, current chemotherapeutic modalities still cause undesirable toxicity in non-tumor cells; thus, improvement in tumor selectivity and therapeutic efficacy has been a major goal in current strategies. Immune conjugation, applications of magnetic field, gene delivery and prodrug approaches for transporters and enzymes have been investigated to increase tumor selectivity (1–8). Prodrug approaches have been extensively utilized to achieve improvement of oral drug delivery, therapeutic efficacy and drug targeting. Gemcitabine, irinotecan and capecitabine are prodrug forms of useful chemotherapeutic agents. Capecitabine is an oral prodrug of 5-fluorouracil (5-FU) and is sequentially converted to 5-FU by select enzymes upon permeation across the intestinal walls. 5-FU, an antitumor agent used in the treatment of solid tumors in breast, colorectal, and gastric cancers is poorly tumor selective and causes high incidences of toxicity in bone marrow, gastrointestinal tract, central nervous system and skin. Capecitibine was therefore developed to improve the tolerability and intratumor drug concentrations through tumor-specific conversion to the active drug (9,10). The elevated levels of 5-FU in plasma suggest metabolism of capecitabine in non-target sites decreases drug targeting to cancer tissues with the liver playing an important role in 5-FU metabolism and elimination (11). Stabilization of the

glycosidic bond and preventing metabolism to 5-FU before reaching tumor sites may enhance its clinical efficacy.

Floxuridine, 5-fluoro-2′-deoxyuridine, is an anticancer agent used clinically in the treatment of colorectal cancers. The mechanistic pathways of floxuridine and its active metabolite 5-FU for anti-tumor effect are well described (12). It has been reported that the potency of floxuridine is higher than that of 5-FU (13). Therefore, stabilizing the glycosidic bond in floxuridine is important and would lead to more efficient cancer therapy. Attachment of an amino acid or dipeptide to 5′-position of floxuridine stabilized its glycosidic bond (14). Gemcitabine, a clinically used cytotoxic agent, is considered as the first-line therapy for pancreatic cancer treatment as well as a wide range of solid tumors including non-small-cell lung cancer (NSCLC) and small-cell lung cancer (SCLC) (15). Gemcitabine has a unique process of self-potentiation inside of cells, high affinity for the gemcitabine metabolic enzyme, increased membrane permeability, longer intracellular retention, and high concentrations of drug in cancer cells (16–19). Antimetabolites like gemcitabine and floxuridine are rapidly distributed throughout body water after intravenous infusion. For increasing therapeutic efficacy, amino acid ester prodrugs of gemcitabine and floxuridine have been synthesized and tested for their affinities to transporters. These prodrugs demonstrated better membrane permeability due to the good affinity to PEPT1 transporters in monolayer cell culture studies and better chemical and enzymatic stabilities *in vitro* (14,20–22).

In vitro models provide a well-defined environment for cancer studies in contrast to the complex host environment of an *in vivo* model. Monolayer cell culture has been popular in *in vitro* models to evaluate the membrane permeability and the growth-inhibitory effects of chemotherapeutic test agents for various cancer studies for years (14,20,23–28). These experiments furnish a great deal of information on the mechanism of drug action and improvements in terms of drug targeting delivery. However, monolayer cell cultures that are two-dimensional may not simulate tissue structural models well to assess chemotherapeutic phenomena *in vivo* because tumor cells that grow faster than non-tumor cells are three-dimensional structures. In fact, it has been reported that one of the disadvantages in an ordinary two-dimensional culture system is the inability to estimate the cell penetration of chemotherapeutic agents *in vivo* (29–32). There also have been numerous reports indicating that traditional monolayer cultures significantly overestimate the sensitivity of cytotoxic treatments (31–33) and 3-D cultures provide the more accurate estimation for *in vivo* studies (34,35). Therefore, the aggregates formed *in vitro* have been utilized to evaluate tumor targeting characteristics (36–38). These aggregates, termed spheroids, mimic the three-dimensional nature of tumors and also present morphological, functional, and mass transport features that are absent in monolayer models (39–41). Thus, three-dimensional tumor models are more physiologically relevant research platforms than monolayer cultures and have been reported to mimic tumor behavior more effectively than two-dimensional monolayer studies (32,42). The development of these *in vitro* culture systems which imitate structural architecture is essential to the design of novel anticancer therapeutics and is invaluable in testing therapeutics in a biologically relevant context for chemotherapeutic treatments (43). In spite of the importance of the three-dimensional cell environment, most studies have not addressed drug delivery to inner tumor sites (39,44) and the quantitation of chemotherapeutic agents and their metabolites for improved chemotherapy (42).

In this report, we introduce a simple two-tier cell culture system to evaluate the potential of prodrug strategies by measuring the membrane permeability of chemotherapeutic agents and quantitating those agents and their metabolites. The ability of floxuridine prodrugs to penetrate tumor cells was investigated in uptake, and their therapeutic efficacy was examined in tumor growth inhibition studies using a simple two-tier monolayer cell model. The ability of amino acid and dipeptide monoester prodrugs of floxuridine to inhibit growth of the secondary (lower) monolayer of Capan-2 cells following permeation across the primary Capan-2 monolayer was examined and compared with the corresponding efficacies of the parent drug. We demonstrated the advantages of floxuridine prodrugs to access inner layers of tumors in association with their forms. The results of these *in vitro* studies might provide insights into drug permeation and bioconversion/bioevasion characteristics in cancer tissues and might improve prediction *in vivo*.

MATERIALS AND METHODS

Materials

Floxuridine was obtained from Lancaster (Windham, NH). The tert-butyloxycarbonyl (Boc)-protected amino acids Boc-L-isoleucine, Boc-L-glycine, Boc-L-valine, Boc-D-valine, Boc-L-phenylalanine, Boc-D-phenylalanine, Boc-L-lysine, Boc-L-leucine, Boc-L-glycyl-L-leucine, Boc-L-phenylalanalyl-L-glycine, Boc-L-leucyl-L-glycine, Boc-L-isoleucyl-L-glycine, Boc-L-valyl-L-phenylalanine, and Boc-L-phenylalanyl-L-tyrosine were obtained from Chem-Impex (Wood Dale, IL). Acetonitrile, high-performance liquid chromatography (HPLC) grade and liquid chromatography-mass spectrometry (LC-MS) grade, was obtained from Fisher Scientific (St. Louis, MO). N,N-dicyclohexylcarbodiimide (DCC), N,N-dimethylaminopyr-

idine (DMAP), and trifluoroacetic acid (TFA) and all other reagents and solvents were purchased from Aldrich-Aldrich Chemical Co. (Milwaukee, WI). Cell culture reagents were obtained from Invitrogen (Carlsbad, CA), and cell culture supplies were obtained from Corning (Corning, NY) and Falcon (Lincoln Park, NJ). All chemicals were either analytical or HPLC grade.

Floxuridine Prodrug Synthesis

The synthesis and characterization of 5′-mono amino acid and 5′-dipeptide ester prodrugs of floxuridine have been reported previously (14,45,46). Amino acid and dipeptide monoester prodrugs of floxuridine were synthesized in a similar manner. Briefly, Boc-protected amino acids or dipeptides (1.1 mmole), DCC (1.1 mmole), and DMAP (0.1 mmole) were allowed to react with floxuridine (1 mmole) in 7 mL of dry DMF for 24 h. The reaction progress was monitored by TLC (ethyl acetate), and DMF was removed under vacuum at 40°C. The residue was extracted with ethyl acetate (30 mL) and washed with water (2×20 mL) and saturated NaCl (20 mL). The organic layer was dried over $MgSO_4$ and concentrated under vacuum. The reaction yielded a mixture of 3′-amino acid/dipeptide monoester, 5′-amino acid/dipeptide monoester, and 3′,5′-amino acid/dipeptide diester floxuridine prodrugs. The three spots observed on TLC were separated (dichloromethane (DCM)/methanol, 20:1, *v*/*v*) and purified using a preparative HPLC purification system. Fractions from each spot were concentrated under vacuum separately. The Boc group was cleaved by treating the residues with 5 mL TFA: DCM (1:1, *v*/*v*). After 4 h, the solvent was removed and the residues were reconstituted with water and lyophilized. The TFA salts of amino acid prodrugs of floxuridine were obtained as white fluffy solids (Fig. 1). The combined yield of floxuridine prodrugs was ~60%. HPLC was used to evaluate the prodrug purity. Prodrugs were between 90% and 99% pure. These prodrugs were easily separated from parent drug by HPLC. Electrospray ionization mass spectra (ESI-MS) were obtained on a Micromass LCT ESI-MS. The observed molecular weights of all prodrugs were found to be consistent with that required by their structure. The structural identity of the prodrugs was then confirmed using proton nuclear magnetic resonance spectra (^{1}H NMR). ^{1}H NMR spectra were obtained on a 300 MHz Bruker DPX-300 NMR spectrometer.

Cell Culture

Capan-2 cells (passages 35–45) from American Type Culture Collection (Rockville, MD) were routinely maintained in RPMI-1640 containing 10% fetal bovine serum at 5% CO_2 and 90% relative humidity at 37°C. Cells were grown in antibiotic-free media to avoid the possible transport interference by antibiotics.

Hydrolysis Studies

Chemical Stability

The non-enzymatic stability of the prodrugs in MES buffer (pH 5.0 and pH 6.0) was determined using the procedure below. MES buffer (250 μL) was added to each well in triplicate, and substrate was added to initiate the reactions that were conducted at 37°C for 8 h. At various time points, aliquots (35 μL) were removed and added to 150 μL of cold ACN containing 0.1% TFA. The mixtures were filtered with a 0.45 μm filter at 1,000 g for 10 min at 4°C. The filtrate was then analyzed *via* reverse-phase HPLC.

Cell Culture Studies

A two-tier monolayer system consisting of Capan-2 cell monolayers was used in this study to determine the ability of floxuridine prodrugs to access the second monolayer following permeation across the first monolayer. The first monolayer was grown on PET (Polyethylene terephthalate) membrane transwell inserts, and the second monolayer was grown at the bottom of a 24-multiwell plate (Fig. 2). The transwell inserts were then placed within each well of the 24-multiwell plate and transport and uptake studies were sequentially performed (Fig. 3). Cell proliferation assays were conducted separately using drug solutions that had permeated across the first monolayer. This simple two-tier *in vitro* model may reveal the potential of floxuridine prodrugs in penetrating tumors.

Transport Studies

Capan-2 cell monolayers were grown on PET membrane inserts of 24-multiwell plates for 14–16 days (growth area of 0.33 cm^2). Transepithelial electrical resistance (TEER) was monitored, and values of 150–200 Ω/cm^2 in Capan-2 were used in the study. The apical and basolateral sides of transwell inserts were washed with MES (pH 5.0) and MES (pH 6.0) buffer, respectively. Fresh MES buffers were reapplied to transwell inserts and incubated at 37°C for 15 min. Freshly prepared 0.1 mM drug solution in MES buffer (pH 5.0, total 0.1 mL) was placed in the donor chamber, and the receiver chamber was filled with MES buffer (pH 6.0, total 0.6 mL). The transwell insert with cells and any unpermeated drug solution was removed at 4 h, and two 100-μL aliquots were sampled from the basolateral (receiver) solution (one for drug assay and the other for cell proliferation studies). Drug assay samples were immediately acidified with 0.1% TFA to

Fig. 1 Structures of mono amino acid and dipeptide ester prodrugs of floxuridine.

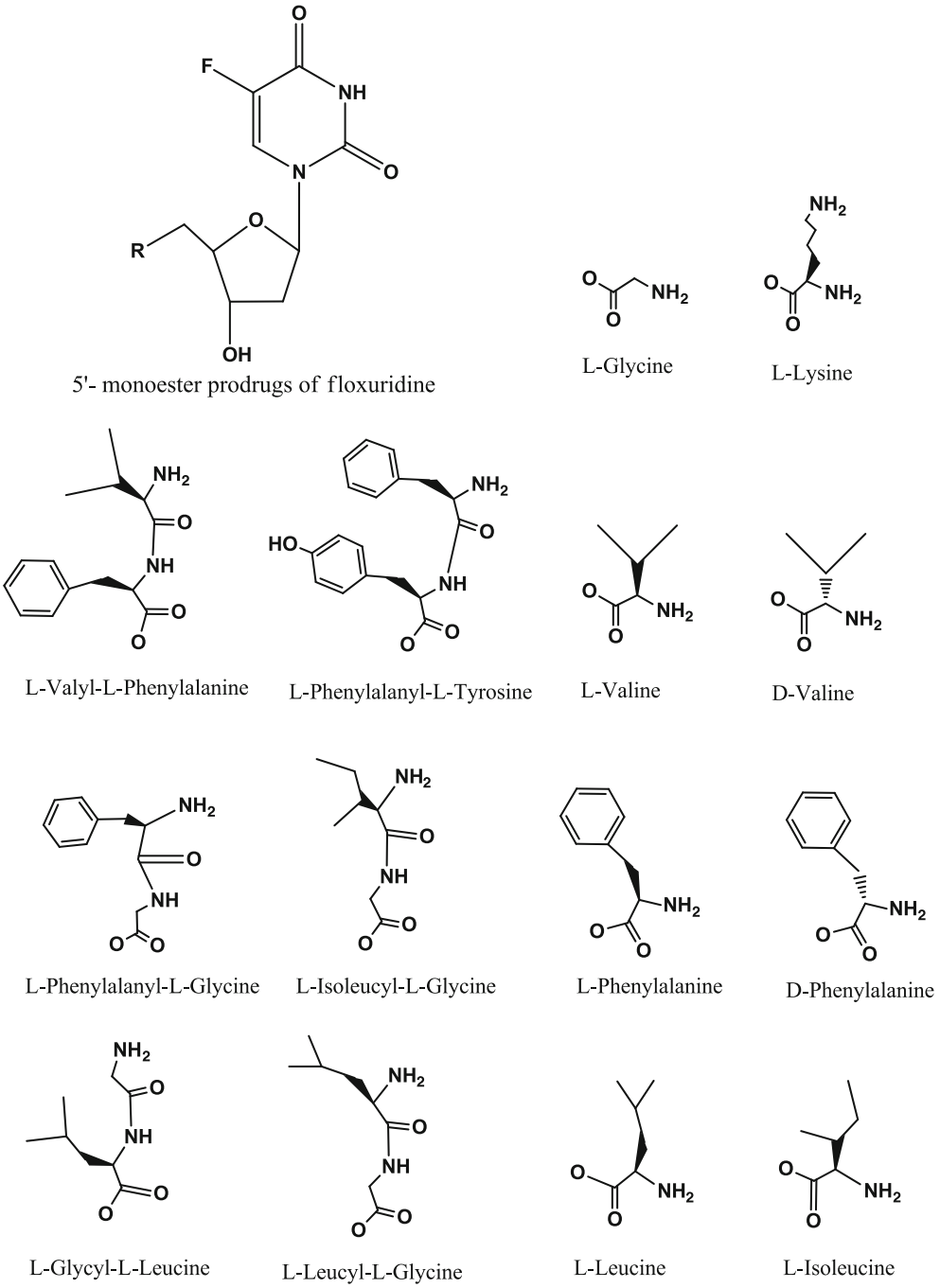

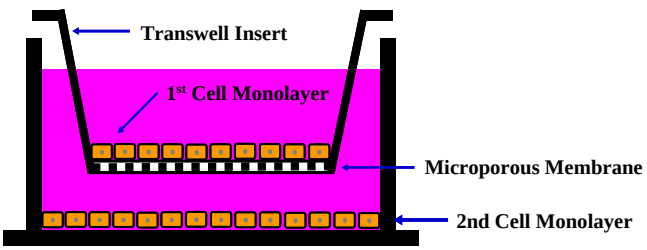

Fig. 2 Schematic of two-tier Capan-2 cell monolayer system. The first Capan-2 monolayer was grown on a PET membrane transwell insert for 14–16 days, and the second monolayer was grown at the bottom of a 24-multiwell plate for 6 days.

stabilize their stabilities and analyzed by reverse-phase HPLC.

Uptake Studies

One thousand cells per well were seeded and allowed to attach/grow for 6 days on 24-multiwell plates prior to transepithelial study (growth area of 2 cm^2). Following the 4 h transport study across the first monolayer and after removal of the transwell inserts and 200 µL of basolateral solution, incubation of the remainder of the

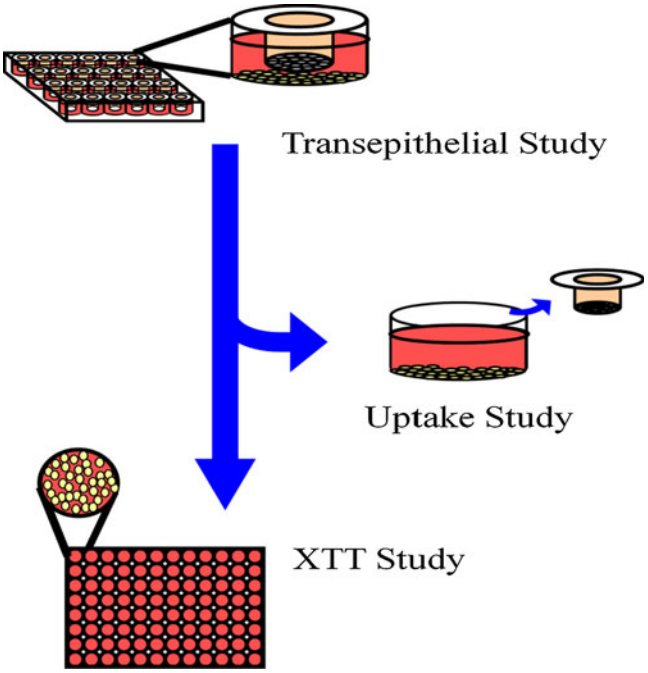

Fig. 3 Schematic of sequential studies of permeation across first layer, uptake in second layer and cell proliferation assays on secondary Capan-2 cells. Permeabilty studies were performed at 37°C for 4 h. One hundred microliters of basolateral chamber solution were transferred to 96-well plates for cell proliferation assays. The remaining sample solution in basolateral chambers was incubated at 37°C for an additional 4 h for uptake studies on the 2nd Capan-2 cell layer (total exposure of 8 h).

400 µL of permeant drug sample in MES buffer (pH 6.0) was continued at 37°C for another 4 h (Fig. 3). At the end of the additional 4 h incubation (total time of 8 h exposure of 2nd monolayer to permeants) all drug solution was removed, and cells were washed three times with ice-cold PBS. Two hundred µL of Milli-Q water/methanol (50:50) were added, and cells were collected in an eppendorf tube. Cell lysate was vortexed and centrifuged for 10 min at 10,000 g at 4°C. The supernatant was treated with ammonium hydroxide (final concentration of 3–5%) to convert all prodrugs to floxuridine and assayed for floxuridine and/or 5-FU content by LC-MS.

Cell Proliferation Assays

Cell proliferation studies were conducted with Capan-2 cell line. The cells were seeded onto 96-well plates at 250 cells per well and allowed to attach/grow for 72 h before drug solutions were added. (A much lower seeding density (250 cells) for second layer proliferation assay was necessitated due to the observation that this was the lowest seeding density where a linear correlation between cell numbers and color change could be obtained in XTT assays.) The culture medium (RPMI-1640 + 10% fetal bovine serum) was removed, and the cells were gently washed once with sterile pH 6.0 uptake buffer. The wash buffer was removed, and 100 µL drug solution sampled from basolateral chamber (as described above) was added to each well and incubated with Capan-2 cells at 37°C for 4 h in a cell incubator (Fig. 3). Buffer alone was used as 100% viability control. After this time period, the drug solutions were removed, and the cells were gently washed twice with sterile uptake buffer. Fresh culture medium was then added to each well after washing, and the cells were allowed to recover for 24 h before evaluating cell viability *via* 2,3-bis[2-methoxy-4-nitro-5-sulfophenyl]-2H-tetrazolium-5-carboxanilide inner salt (XTT) assays. A mixture (30 µL) containing XTT (1 mg/mL) in sterile RPMI-1640 without phenol red and phenazine methosulfate (N-methyl dibenzopyrazine methyl sulfate in sterile PBS, 0.383 mg/mL) reagents was added to the cells and incubated at 37°C for 1 h, after which the absorbance at 450 nm was read. The percentage of growth inhibition was then calculated.

Data Analysis

The initial rates of hydrolysis were used to obtain the apparent first-order rate constants and to calculate the half-lives. The apparent first-order degradation rate constants of various floxuridine prodrugs at 37°C were determined by plotting the logarithm of prodrug remaining as a function of time. The slopes of these plots are related to the rate constant, k, and given by

$$\mathrm{k} = 2.303 \times \mathrm{slope}(\ \log \mathrm{C}\ \textit{vs.}\ \mathrm{time}) \tag{1}$$

The degradation half-lives were then calculated by the equation,

$$\mathrm{t}_{1/2} = 0.693/\mathrm{k} \tag{2}$$

The apparent permeability (P_{app}) for the prodrugs was calculated using the following equations:

$$Flux = J_{ss} = dM/dt \tag{3}$$

where J_{ss} is the steady state flux, M is the cumulative amount of prodrug, regenerated mono amino acid prodrug, drug and 5-FU in the receiver compartment. The apparent permeability was calculated from steady-state flux as follows:

$$P_{app} = \frac{J_{ss}}{A \times C_0} \tag{4}$$

where A is the surface area of monolayer exposed to the permeant, and C_0 is the concentration of the prodrug in the

donor solution. The concentrations of floxuridine and its prodrugs in the receiver and donor compartments were analyzed using HPLC.

Regression analyses were carried out with Microsoft Office Excel 2007 software using mean values. Statistical significance of correlation coefficients was evaluated using ANOVA. Comparisons for statistical significance were carried out using Student's *t*-tests. All *p* values cited are for two-tailed (or non-directional) tests, and a *p* value of <0.05 was considered significant.

HPLC Analysis

The cell-permeated amounts of prodrugs and their metabolites were determined on an Agilent HPLC system (Agilent Technologies, Santa Clara, CA). The HPLC system consisted of Agilent pumps (1100 series), an Agilent autosampler (1200 series), and an Agilent UV–vis detector (1100 series) controlled by Chemstation® 32 software (version B.01.03). Samples were resolved in an Agilent Eclipse Plus C_{18} reverse-phase column (3.5 μm, 4.6×75 mm) equipped with a guard column. The mobile phase consisted of 0.1% TFA/water (Solvent A) and 0.1% TFA/acetonitrile (Solvent B) with the solvent B gradient changing from 0% to 56% at a rate of 2%/min during a 20 min run for floxuridine. Standard curves generated for each prodrug and their parent drugs were utilized for quantitation of integrated area under peaks. Similar standard curves were used to quantitate mono amino acid ester prodrugs metabolized from dipeptide ester prodrugs. The detection wavelength was 254 nm and spectra were acquired in the 220–380 nm range.

Preparative HPLC Purification System

The purification of synthesized test compounds was performed on a Shimadzu preparative HPLC system (Shimadzu Scientific Instruments, Kyoto, Japan). The Shimadzu preparative HPLC system consisted of two Shimadzu pumps (model LC-8A) with Shimadzu system controller (model SCL-10A), a Shimadzu prominence diode array (PDA) detector (model SPD-M20A) with a 10 mL sample loop controlled by LCsolution software (version 1.23). Samples were resolved in a Waters XBridge™ C_{18} reverse-phase column (5 μm, 30× 250 mm, Milford, MA, USA) for preparative separation. The mobile phase consisted of 0.1% TFA/water (Solvent A) and 0.1% TFA/acetonitrile (Solvent B) with the solvent B gradient changing from 5% to 90% at a rate of 2%/min over a 30 min run. The flow rate was 15 mL/min, and the injection volume was 0.5 mL. The detection wavelengths were 254 nm and 275 nm.

LC-MS Analysis

LC-MS analysis of the uptake drug amount was performed in triplicate on LCMS-2010EV (Shimadzu Scientific Instruments, Kyoto, Japan) equipped with an ESI (electrospray ionization) source. The Shimadzu LC-MS system consisting of a Shimadzu LC-20AD pump with DGU-20A in-line vacuum degasser units, and SIL-20HT autosampler with a Restek C-18 column (5 μm, 50×2.1 mm) was used for the separation, and the effluent from the column was directly to the ionization source. The system was controlled by Shimadzu LCMS solution software (version 3) to collect and process data. All samples were run with Solvent A and Solvent B (described earlier) with Solvent B gradient changing from 0% to 90% at a rate of 13.8%/min over a 22 min run. The ESI probe was operated with a detector voltage of 1.5 kV, CDL temperature of 250°C, heat block of 200°C, and nebulizing gas flow of 1.2 mL/min in negative mode for 5-FdUrd and 5-FU, and in positive mode for floxuridine prodrugs. The drying gas was N_2 delivered at 0.1 MPa.

RESULTS

Floxuridine Prodrugs

The synthesis of the prodrugs and their characterization have been described in previous reports (14,20,45,46). The structures of those prodrugs are shown in Fig. 1.

Stability Studies

The experiments of prodrug stability were performed at 37°C in pH 5.0 and pH 6.0 MES buffers. The percentages of drug or prodrug recovered following incubation of the test substances in pH 5.0 and pH 6.0 MES buffers are listed in Table I. Half-lives are not reported since the observed chemical degradation over 8 h experimental time period was comparatively too small to allow reliable estimations using pseudo-first order plots. No chemical degradation was evident with all tested floxuridine prodrugs in pH 5.0 MES buffer. In pH 6.0 MES buffer all tested prodrugs showed no degradation except for the three leucine-containing prodrugs. 5′-O-L-leucyl-floxuridine, 5′-O-L-leucyl-L-glycyl-floxuridine, and 5′-O-L-glycyl-L-leucyl-floxuridine exhibited less than 6.0% of prodrug loss in pH 6.0 MES buffer over 8 h. Thus, all tested prodrugs would be expectedly stable in pH 5.0 and pH 6.0 MES buffers during entire experiment. The stability of floxuridine-3′-L-proline, a stable prodrug, was also tested as a control in pH 5.0 and 6.0 MES buffers, and no degradation was observed.

Table I Stability of Prodrugs in Buffers

Prodrug	Percent prodrug recovery at 8 h	
	pH 5.0 MES buffer	pH 6.0 MES buffer
Floxuridine	100.0 ± 1.2	100.0 ± 1.6
5′-O-L-lysyl-floxuridine	106.6 ± 2.7	101.2 ± 2.2
5′-O-L-leucyl-floxuridine	100.9 ± 0.8	***94.7 ± 7.6***
5′-O-L-glycyl-floxuridine	102.7 ± 2.4	106.5 ± 7.5
5′-O-L-valyl-floxuridine	102.3 ± 2.7	102.1 ± 1.4
5′-O-D-valyl-floxuridine	103.4 ± 5.3	102.3 ± 6.4
5′-O-L-isoleucyl-floxuridine	102.0 ± 1.5	101.0 ± 1.2
5′-O-L-phenylalanyl-floxuridine	101.9 ± 1.3	103.7 ± 3.5
5′-O-D-phenylalanyl-floxuridine	101.5 ± 1.3	103.5 ± 3.8
5′-O-L-leucyl-L-glycyl-floxuridine	105.2 ± 4.2	***98.6 ± 2.0***
5′-O-L-glycyl-L-leucyl-floxuridine	105.5 ± 5.4	***94.6 ± 8.8***
5′-O-L-phenylalanyl-L-tyrosyl-floxuridine	109.0 ± 5.6	104.1 ± 3.3
5′-O-L-phenylalanyl-L-glycyl-floxuridine	101.4 ± 2.1	105.1 ± 6.4
5′-O-L-valyl-L-phenylalanyl-floxuridine	103.2 ± 2.0	101.1 ± 0.4
5′-O-L-isoleucyl-L-glycyl-floxuridine	104.1 ± 1.3	103.6 ± 4.1
Floxuridine-3′-L-proline	104.6 ± 1.0	102.9 ± 2.2

Mean ± SD, $n = 6$

Permeability Studies

The extent of permeation of monoamino acid/dipeptide monoester prodrugs of floxuridine and parent floxuridine across the first Capan-2 monolayers were determined over a 4-h period at 37°C. During this series of experiments, metabolic degradations of starting materials in donor compartment were not big but were observed, indicating drug/prodrug hydrolysis by cell membrane associated enzymes (data not shown). Mass balance was not achieved because 5-FU was metabolized further, and those metabolites beyond 5-FU were not quantified by HPLC. Table II shows the amounts of intact prodrugs as well as their enzymatic degradation products such as 5-FU and monoamino prodrugs found in the basolateral compartment 4 h following permeation across the first monolayer. The results are also shown in Fig. 4 for ease of comparison. Although floxuridine permeated Capan-2 cells, only its metabolite was found in the basolateral chamber. The total concentration of prodrugs and enzymatic degradation products were 4- to 10-fold higher than the concentrations obtained with parent floxuridine for all floxuridine prodrugs tested except for 5′-O-L-leucyl-floxuridine (1.5-fold higher). Floxuridine was not detected in the basolateral chamber with any tested prodrugs suggesting that the glycosidic bond of floxuridine was rapidly degraded by metabolic enzymes such as thymidine phosphorylase in Capan-2 cells. With the exception of 5′-O-L-lysyl-floxuridine and 5′-O-L-glycyl-floxuridine, which were nearly completely metabolized to 5-fluorouracil after permeation (100% 5-FU and 98% 5-FU, respectively), varying amounts of intact prodrugs were found with the other prodrugs tested. Thus, for mono amino acid prodrugs, an average of 45.5% of the permeated amounts was found intact in the basolateral chamber after 4 h (range 34.4–62.5%). An average of 48.4% of the dipeptide prodrugs (range 13.0–97.8%) was found intact in the basolateral chamber 4 h following permeation across the first Capan-2 monolayer. The amounts of mono amino acid prodrugs found as intermediate metabolites from dipeptide prodrugs were negligible (average 1.8%; range 0–4.3%). The total amounts of prodrugs and metabolites permeating the first monolayer were highest for 5′-O-L-phenylalanyl-L-glycyl-floxuridine; however, only 16.5% of the permeated drug in basolateral side remained intact. On the other hand, 97.8% of 5′-O-L-phenylalanyl-L-tyrosyl-floxuridine remained intact in basolateral side after permeating the first Capan-2 cell monolayer.

Uptake Studies

The uptake amounts in the second monolayer were determined following incubation with permeants of various prodrugs and parent floxuridine that had traversed the first Capan-2 monolayer. The total incubation time was 8 h, 4 h with the transwell insert containing first monolayer in place and an additional 4 h after removal of the transwell insert. The uptake of drug in the second Capan-2 monolayer was assayed by LC-MS using standard curves constructed with known concentrations of floxuridine and 5-fluorouracil. Since the samples were treated with strong base prior to

Table II Composition of Basolateral Solution 4 h Following Transport of Floxuridine Prodrugs Across First Capan-2 Monolayer

Compound	Composition, μM			Composition percentage		
	5-FU	Monoamino acid prodrug	Dipeptide prodrug	% 5-FU	% Mono	% Dipeptide
Floxuridine	0.117 ± 0.002			100.0		
5′-O-L-Lysyl-Floxuridine	0.689 ± 0.095	0 ± 0		100.0	0.0	
5′-O- L-Leucyl-Floxuridine	0.066 ± 0.010	0.110 ± 0.010		37.5	62.5	
5′-O- L-Glycyl-Floxuridine	0.865 ± 0.104	0.018 ± 0.001		98.0	2.0	
5′-O- L-Valyl-Floxuridine	0.443 ± 0.024	0.286 ± 0.026		60.8	39.2	
5′-O-D-Valyl-Floxuridine	0.412 ± 0.022	0.496 ± 0.035		45.4	54.6	
5′-O-L-Isoleucyl-Floxuridine	0.333 ± 0.032	0.175 ± 0.005		65.6	34.4	
5′-O-L-Phenylalanyl-Floxuridine	0.481 ± 0.095	0.317 ± 0.085		60.3	39.7	
5′-O-D-Phenylalanyl-Floxuridine	0.301 ± 0.030	0.220 ± 0.005		57.8	42.2	
5′-O-L-Leucyl-L-Glycyl-Floxuridine	0.506 ± 0.060	0.021 ± 0.001	0.432 ± 0.017	52.8	2.2	45.0
5′-O-L-Glycyl-L-Leucyl-Floxuridine	0.584 ± 0.034	0 ± 0	0.352 ± 0.042	62.4	0.0	37.6
5′-O-L-Phenylalanyl-L-Tyrosyl-Floxuridine	0.004 ± 0.008	0.012 ± 0.002	0.711 ± 0.031	0.5	1.7	97.8
5′-O-L-Phenylalanyl-L-Glycyl-Floxuridine	1.033 ± 0.168	0.014 ± 0.001	0.156 ± 0.005	85.9	1.1	13.0
5′-O-L-Valyl-L-Phenylalanyl-Floxuridine	0.480 ± 0.048	0.016 ± 0.001	0.480 ± 0.048	49.2	1.6	49.2
5′-O-L-Isoleucyl-L-Glycyl-Floxuridine	0.406 ± 0.021	0.021 ± 0.003	0.233 ± 0.039	61.5	3.2	35.3

Mean ± SD, $n = 3$.

assay, only floxuridine or 5-FU was detected. The results, shown in Fig. 5, indicate that uptake of the parent floxuridine was not detected in the 2nd monolayer. However, uptake of all prodrugs of floxuridine tested was observed in the second Capan-2 monolayer. The highest uptake amounts in the second layer of Capan-2 cells, 288 ± 60 pg and 242 ± 136 pg, were observed with 5′-O-L-valyl-floxuridine and 5′-O-L-phenylalanyl-L-tyrosyl-floxuridine,

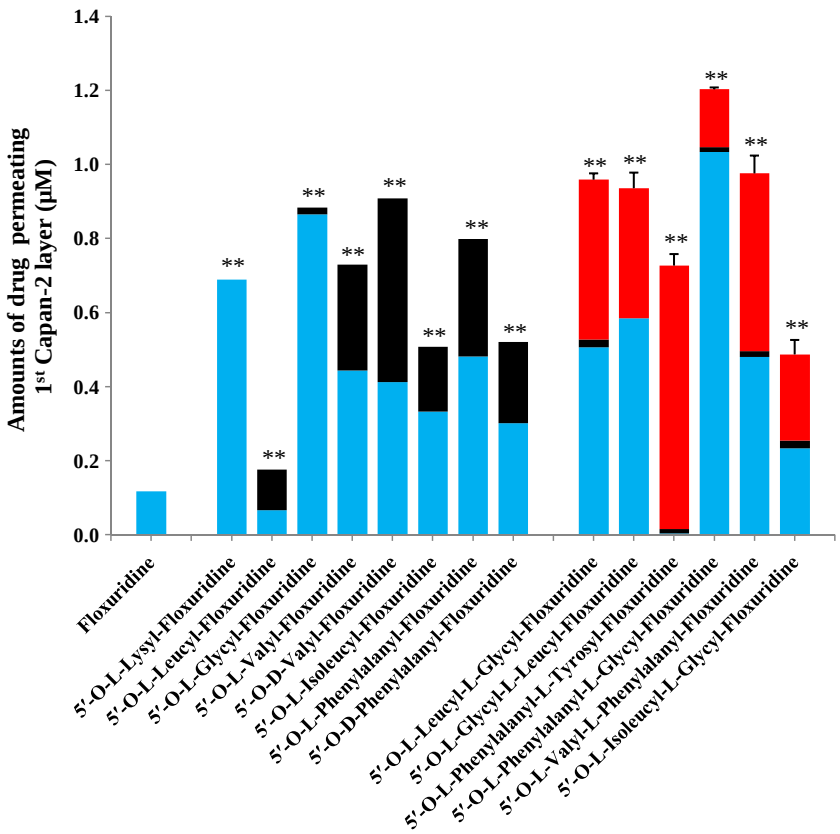

Fig. 4 Amounts of floxuridine and floxuridine prodrugs found in basolateral compartment at 4 h following permeation across first monolayer of Capan-2 cells. Blue column represents 5-fluorouracil, black column represents mono amino acid ester prodrug form, and red column represents dipeptide monoester prodrug form. Data are expressed as micromoles of prodrug form, mean ± S.D., $n = 3$–6. Error bars are shown only for dipeptide prodrug form to avoid cluttering of the graphical representation (all S.D. values listed in Table II).

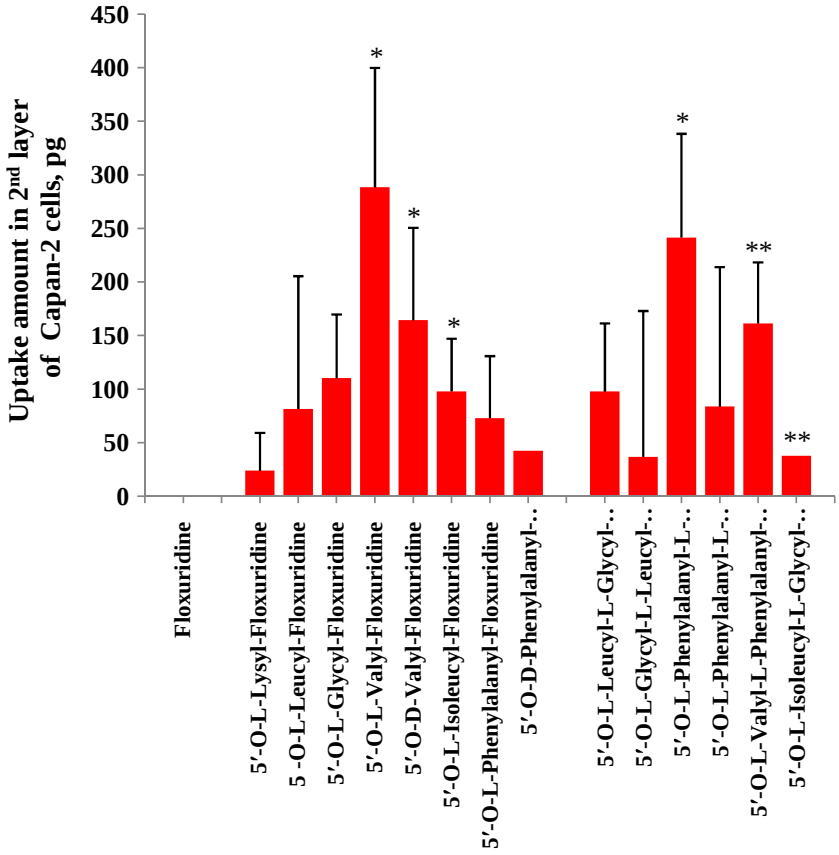

Fig. 5 Uptake amounts in second monolayer of Capan-2 cells determined at 8 h following permeation of floxuridine and floxuridine prodrugs across first Capan-2 monolayer. The drug amounts were measured as floxuridine and/or 5-fluorouracil. Data are expressed as picograms floxuridine and/or 5-FU, mean ± S.D., $n = 3–6$.

respectively. The uptake amounts in the second monolayer exhibited a very poor linear correlation ($r^2 = 0.01$) with the total amounts of drug (combined amounts of intact prodrug and its enzymatic degradation products) present in the basolateral compartment 4 h following permeation across the first monolayer. The linear correlation of uptake amounts in the second monolayer is stronger and significant when only amounts of intact prodrug or prodrug forms are used ($r^2 = 0.30$, two-tailed $p = 0.04$). If mono amino acid prodrugs and dipeptide prodrugs are evaluated separately, this linear correlation significantly improves for dipeptide prodrugs ($r^2 = 0.74$, $p = 0.02$); however, the correlation of uptake amounts with intact prodrug forms of mono amino acid prodrugs gets weaker and insignificant ($r^2 = 0.22$, $p = 0.24$) (Fig. 7).

Cell Proliferation Assay

The ability of floxuridine prodrugs to inhibit growth of the second layer of Capan-2 cells was determined in a separate study. Thus, receiver solutions obtained at 4 h following permeation of various floxuridine prodrugs across the first Capan-2 monolayer (described in Transport Study section above) were incubated with a secondary Capan-2 monolayer. The Capan-2 monolayers used in these studies were grown at a much lower seeding density of 700 cells per well in order to elicit differences between the various prodrugs and since a linear correlation between absorbance and cell number could not be obtained in XTT assays at lower seeding densities. The percentages of cell growth inhibition observed with floxuridine and its 5′-mono amino acid/dipeptide monoester prodrugs determined in these cell proliferation studies are shown in Fig. 6. It is evident that the extent of growth inhibition observed is quite low, ranging between 0% and 9%. Growth inhibition was not observed with floxuridine and with the prodrugs 5′-O-L-lysyl-floxuridine, 5′-O-L-glycyl-floxuridine, 5′-O-L-isoleucyl-floxuridine, 5′-O-D-phenylalanyl-floxuridine, and 5′-O-L-phenylalanyl-L-glycyl-floxuridine. Permeant solutions of 5′-O-L-valyl-floxuridine and 5′-O-L-leucyl-L-glycyl-floxuridine exhibited the highest extent of growth inhibition on the second Capan-2 layer; the percent growth inhibitions from these were 9.0 and 6.4, respectively. The inhibitory activity of tumor cell growth on the second layer was thus reduced due to the limited availability of anti-cancer drugs following permeation across the first Capan-2 cell layers (Fig. 3, 7).

The linear correlation of growth inhibition extent with total drug permeated across the first monolayer at 4 h was

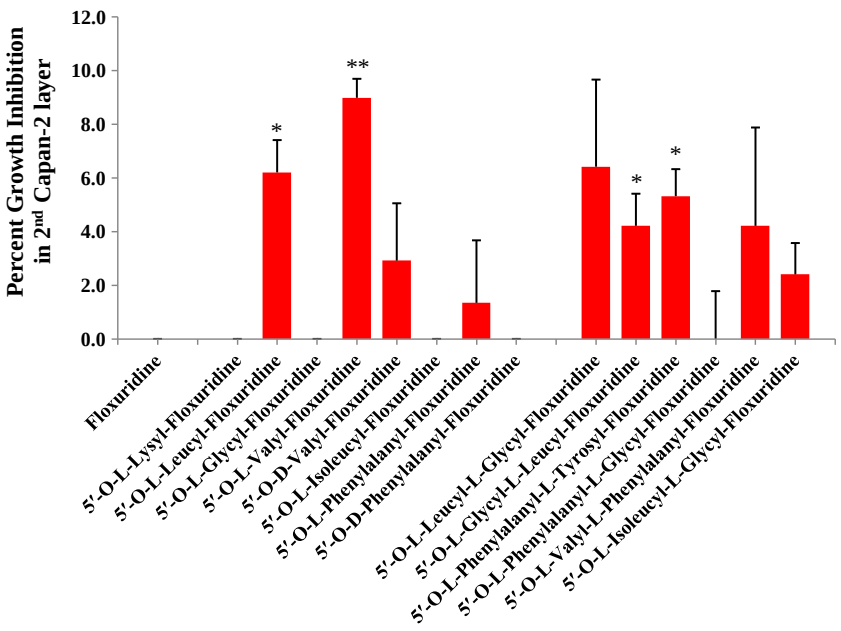

Fig. 6 Percent cell growth inhibition of a secondary Capan-2 layer following incubation with permeant solutions in basolateral compartment obtained at 4 h following permeation of floxuridine and floxuridine prodrugs across first monolayer of Capan-2 cells. Buffer was used as 100% viability control. Data are expressed as mean ± S.D., $n=3–6$.

quite poor ($r^2=0.01$). The correlation, in a manner similar to the correlations observed with uptake in the second layer, improved when only intact prodrug amounts were used in the correlation ($r^2=0.25$, $p=0.07$). Here again, separately evaluating mono amino prodrugs and dipeptide prodrugs showed remarkable differences. For monoamino acid prodrugs, the linear correlation between intact prodrug amounts and growth inhibition was poor ($r^2=0.09$); however, a stronger correlation ($r^2=0.60$, $p=0.07$) was obtained with dipeptide prodrugs. The correlation improves if the logarithm of growth inhibition is plotted *versus* dipeptide prodrug amounts ($r^2=0.77$, $p=0.022$) (plot not shown).

DISCUSSION

Prodrug strategies have been adopted for current anti-infective and anti-cancer agents in efforts to improve drug absorption and efficacy of delivery to target sites. The clinically viable antiviral drugs valacyclovir and valganciclovir are early examples of the successful use of amino acid prodrug approaches to enhance intestinal absorption of poorly permeable drugs (47–52). The improvement of oral bioavailability of these antiviral prodrugs has been attributed to their carrier-mediated-transport by oligopeptide transporters in the gastrointestinal tract (53–56). A variety of promoieties, including amino acids, dipeptides, tripeptides, and their mimetics, have since been investigated for their suitability as substrates for carrier-mediated oligopeptide and amino acid transporters (57–62). We have previously described the transport, enzymatic stability, and *in vitro* antiviral and cytotoxic activity characteristics of amino acid/dipeptide monoester prodrugs of anti-cancer drugs such as floxuridine and anti-virals such as 2-bromo-5,6-dichloro-1-(β-D-ribofuranosyl)benzimidazole (BDCRB) and gemcitabine (14,20,21,45,46,63,64). It was shown that, in general, amino acid and dipeptide monoester prodrugs provided enhanced PEPT1-mediated transport, a wide range of bioactivation rates, and bioevasion of metabolic enzymes such as thymidine phosphorylase (TP), cytidine deaminase (CDA) and dihydropyrimidine dehydrogenase (DPD). Our group has also reported that amino acid/dipeptide monoester prodrugs of anti-cancer drugs exhibited higher permeability, better growth inhibition, and superior stability to enzymes such as thymidine phosphorylase (14,20–22,45).

In this report, a simple two-monolayer *in vitro* tissue culture system with Capan-2 cells (a pancreatic duct cancer cell line) was used a) to examine the ability of amino acid/dipeptide monoester prodrugs of floxuridine to permeate the first monolayer and b) to determine the uptake and cell proliferation characteristics of the permeants in the second monolayer. The two-monolayer set-up used in these studies cannot simulate the cellular architecture, phenotypic variations and other differences that have been detailed in studies using more sophisticated three-dimensional models of tumors. However, this two-layer set-up may reveal both the potential of amino acid/dipeptide prodrugs to permeate into inner layers of tumors and the correlative relationship between drug forms and therapeutic effects (26,37,39,40). Those cannot be determined by traditional monolayer cultures. Thus, the two-tier cell culture system would have advantages in evaluating the efficacy of drug/prodrug at the early stage of development and the

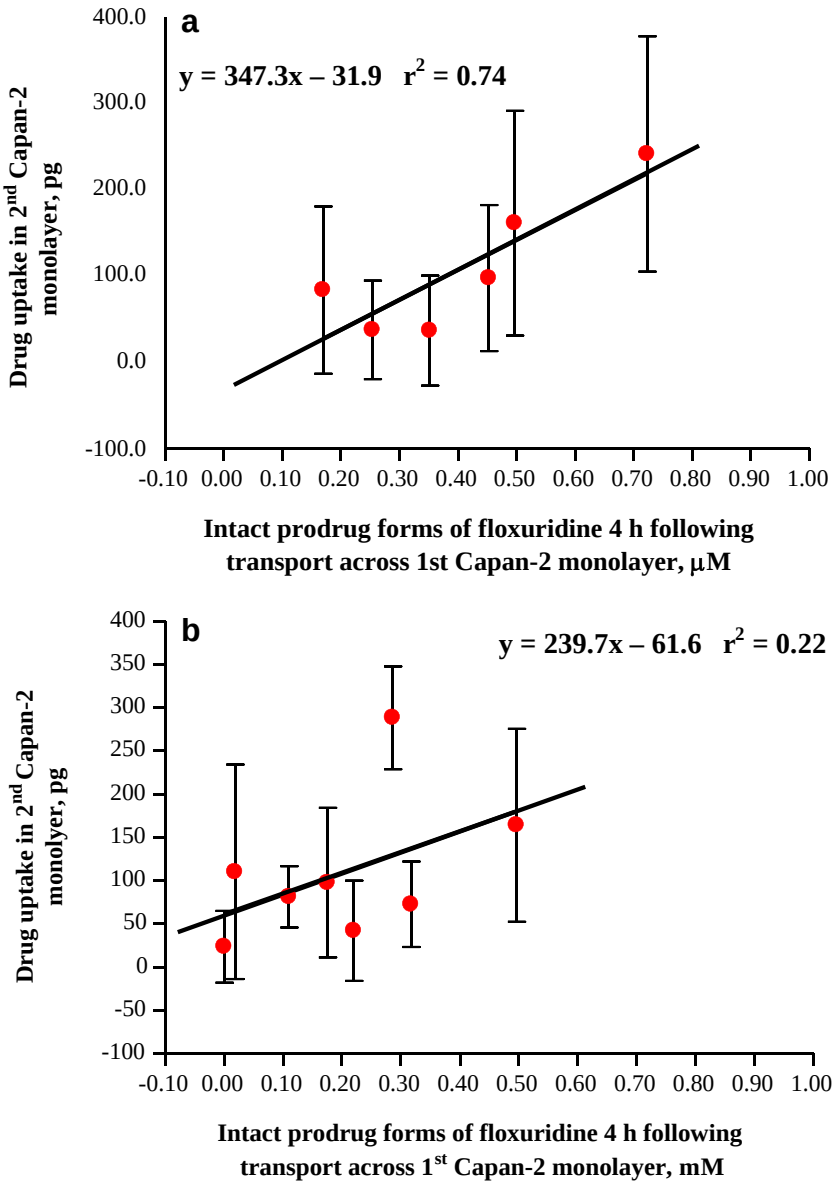

Fig. 7 Linear correlation between uptake amounts in the second layer of Capan-2 cells and intact dipeptide prodrug in basolateral compartment at 4 h for dipeptide monoester floxuridine prodrugs.

appropriate combination of drug/prodrug for a multilayered tumor treatment.

All prodrugs of floxuridine exhibited greater permeation across the first Capan-2 monolayer than the parent drug. The apparent permeability coefficients determined in this study using amounts of total drug permeating the first layer at 4 h did not correlate very well with previously reported apparent permeability coefficients of the prodrugs across Capan-2 monolayers (14). The exponential correlation improved (from $r^2 = 0.35$ to $r^2 = 0.66$) when three prodrugs, 5′-O-L-lysyl-floxuridine, 5′-O-L-isoglycyl-L-glycyl-floxuridine and 5′-O-L-phenyly-L-tyrosyl-floxuridine, were excluded. The poor correlation may be due to inherent differences in cell culture parameters or due to the lack of sampling during the early transport period (0–2 h). The enhanced permeation of the prodrugs compared to the parent drug is, however, consistent with their enhanced affinity and transport by PEPT1 transporter (14,21,22,55,64).

The stability of the tested prodrugs in pH 5.0 and pH 6.0 buffers appear to reflect the trends in chemical stability in pH 7.4 buffer observed earlier (14). Thus, only leucine-containing prodrugs exhibited nominal loss of prodrugs in pH 6.0 MES buffer; the others showed no degradation. Diketopiperazine cyclization is another possible degradation pathway for dipeptide monoester prodrugs. However, it has been reported that the rate of intramolecular aminolysis is neglible at pH values below 6 (14,65,66). Thus, under experimental conditions wherein chemical degradation of tested compounds was minimal, the prodrug

metabolites observed in the basolateral compartment are the result of enzymatic degradation during transport across Capan-2 monolayers.

An average of 45–48% of the prodrugs was found intact in the basolateral compartment 4 h following permeation across the first Capan-2 monolayers. This result suggests that the drug stability in cell homogenates may not reflect the drug stability in permeation. The cleavage of the ester bond of floxuridine prodrugs has been suggested to be the rate-limiting step in determining enzymatic prodrug stability. Floxuridine that is generated from the prodrugs *via* chemical or enzymatic attack is degraded to 5-FU, which is sequentially metabolized further (14). Metabolic enzymes such as thymidine phosphorylase (TP) and dihydropyrimidine dehydrogenase (DPD) in tumor cells such as Capan-2 cells are involved in the catabolism of floxuridine and 5-fluorouracil. Once prodrugs are metabolized to floxuridine, those enzymes would quickly degrade pyrimidine analogues. Thus, up-regulation of metabolic enzymes in cancer cells would reduce apparent drug permeation due to their rapid degradation.

The uptake and cell proliferation studies with a secondary layer of pancreatic duct cancer cell lines corroborate the enhanced cell penetration ability of the amino acid/dipeptide monoester prodrugs of floxuridine compared to parent drug, floxuridine. Uptake of all prodrugs was detected in the second layer of tumor cells, while uptake of floxuridine was not observed. Floxuridine is rapidly metabolized to 5-FU in Capan-2 cells; however, the esterification of the hydroxyl groups prohibits the conversion of floxuridine to 5-FU by protecting the glycosidic bond (14,45). The majority of detected floxuridine in the second monolayer would have been converted from floxuridine prodrugs during sample preparation for LC-MS analysis (Fig. 5). The inhibitory effects of floxuridine prodrugs on the second Capan-2 layer were not as high as ones on the first Capan-2 layer in the previous report (14). This result of the second layer inhibitory effect indicates that traditional monolayer cultures would overestimate the sensitivity of Capan-2 cells to cytotoxic treatments (32,33). The correlation between uptake and growth inhibition in the second monolayer with intact prodrug amounts and the absence of such a correlation with total drug permeating the first monolayer suggests that both permeability and enzymatic stability are essential for sustained action of prodrugs in deeper layers of tumors. The correlation of uptake as well as growth inhibition was vastly superior for dipeptide prodrugs than those obtained with mono amino acid prodrugs. Although the linear correlation of uptake in the second layer with intact prodrug forms was weak, it was statistically significant ($r^2=0.30$; $p=0.04$). The lower potency of prodrugs containing D-amino acids compared to their L-forms (5′-O-D-valyl-floxuridine *vs.* 5′-O-L-valyl-floxuridine, and 5′-O-D-phenylalanyl-floxuridine *vs.* 5′-O-L-phenylalanyl-floxuridine), in the second layer of Capan-2 cells, suggests that activation of the prodrugs to the parent is a necessary step for anti-proliferation activities.

It is evident that none of the prodrugs tested individually provide optimum behavior with respect to permeation across the first monolayer, stability to enzymatic degradation, and uptake/cell proliferation activity in the second layer. It may be possible, however, to achieve optimum action in the two monolayers with a mixture of prodrugs that exhibit the best individual characteristics with respect to permeation across first monolayer, stability to enzymatic degradation, and uptake/cell proliferation activity in second layer. A mixture of 5′-O-L-valyl-floxuridine, 5′-O-L-phenylalanyl-L-glycyl-floxuridine, and 5′-O-L-phenylalanyl-L-tyrosyl-floxuridine is a representative example. The individual characteristics of the three prodrugs in the cocktail are briefly presented below. 5′-O-L-phenylalanyl-L-glycyl-floxuridine exhibited the highest permeation across the first Capan-2 layer but not the highest growth inhibition nor highest uptake with the second Capan-2 cell monolayers. However, 5′-O-L-phenylalanyl-L-glycyl-floxuridine was shown to exhibit good cell growth inhibition in two pancreatic duct cancer cell lines in a previous study (14), suggesting its effectiveness in treating surface layers (the first layer) of multi-layered tumor cells. 5′-O-L-valyl-floxuridine exhibited the highest growth inhibition and uptake with the second Capan-2 cell monolayers even though its permeation across the first layer was not the highest.

5′-O-L-phenylalanyl-L-tyrosyl-floxuridine exhibited the greatest retention of intact prodrug form following permeation across the first Capan-2 monolayers and the second best uptake on the second Capan-2 cell monolayers among tested prodrugs, suggesting its beneficial ability to penetrate into inner tumor layers. 5′-O-L-phenylalanyl-L-tyrosyl-floxuridine also exerted cytotoxic action on the second Capan-2 layer indicating prodrug activation. Thus, assuming independence of transport and enzymatic degradation of the three prodrugs when applied as a mixture, such administration could be effective in the treatment of surface layers and interior layers of multi-layered tumor cells.

CONCLUSIONS

Two-tier culture system could provide the valuable information to design more effective prodrugs and combination of chemotherapeutic treatments. The results of uptake and growth inhibition on the second layer of this two-tier culture system indicate that amino acid/dipeptide monoester prodrugs of floxuridine that remain as intact prodrugs following permeation across the first Capan-2 monolayer

provide enhanced cell penetration and cytotoxic effects on a secondary layer than their metabolites or their parent drug, floxuridine. Therefore, stable prodrugs might facilitate enhanced delivery of active drug to inner layers of tumor cells compared to parent or metabolized prodrugs and, therefore, might possess an advantage for more efficient cancer treatment. The finding that the prodrugs exhibit a wide range of permeability, bioactivation, and anti-proliferation profiles suggests that the application of a mixture of prodrugs (prodrug cocktails) would be more effective in treating multi-layered tumor cells than the application of a single prodrug.

ACKNOWLEDGMENTS

We thank Dr. Wei Shen for his expertise with prodrug purification. This work was supported by grants NIGMD-2R01GM037188.

REFERENCES

1. Bookman MA. Biologic therapies for gynecologic cancer. Curr Opin Oncol. 1995;7:478–84.
2. Gray J, Frith C, Parker J. *In vivo* enhancement of chemotherapy with static electric or magnetic fields. Bioelectromagnetics. 2000;21:575–83.
3. Kamstock D, Guth A, Elmslie R, Kurzman I, Liggitt D, Coro L, *et al.* Liposome-DNA complexes infused intravenously inhibit tumor angiogenesis and elicit antitumor activity in dogs with soft tissue sarcoma. Cancer Gene Ther. 2006;13:306–17.
4. Keler T, Khan S, Sorof S. Liver fatty acid binding protein and mitogenesis in transfected hepatoma cells. Adv Exp Med Biol. 1997;400A:517–24.
5. Kratz F, Mansour A, Soltau J, Warnecke A, Fichtner I, Unger C, *et al.* Development of albumin-binding doxorubicin prodrugs that are cleaved by prostate-specific antigen. Arch Pharm (Weinheim). 2005;338:462–72.
6. Kullberg M, Mann K, Owens JL. Improved drug delivery to cancer cells: a method using magnetoliposomes that target epidermal growth factor receptors. Med Hypotheses. 2005;64:468–70.
7. Mittal S, Song X, Vig BS, Landowski CP, Kim I, Hilfinger JM, *et al.* Prolidase, a potential enzyme target for melanoma: design of proline-containing dipeptide-like prodrugs. Mol Pharm. 2005;2:37–46.
8. Wagner E, Kircheis R, Walker GF. Targeted nucleic acid delivery into tumors: new avenues for cancer therapy. Biomed Pharmacother. 2004;58:152–61.
9. Shimma N, Umeda I, Arasaki M, Murasaki C, Masubuchi K, Kohchi Y, *et al.* The design and synthesis of a new tumor-selective fluoropyrimidine carbamate, capecitabine. Bioorg Med Chem. 2000;8:1697–706.
10. Miwa M, Ura M, Nishida M, Sawada N, Ishikawa T, Mori K, *et al.* Design of a novel oral fluoropyrimidine carbamate, capecitabine, which generates 5-fluorouracil selectively in tumors by enzymes concentrated in human liver and cancer tissue. Eur J Cancer. 1998;34:1274–81.
11. Pinedo HM, Peters GF. Fluorouracil: biochemistry and pharmacology. J Clin Oncol. 1988;6:1653–64.
12. Grem JL, Harold N, Shapiro J, Bi DQ, Quinn MG, Zentko S, *et al.* Phase I and pharmacokinetic trial of weekly oral fluorouracil given with eniluracil and low-dose leucovorin to patients with solid tumors. J Clin Oncol. 2000;18:3952–63.
13. Laskin JD, Evans RM, Slocum HK, Burke D, Hakala MT. Basis for natural variation in sensitivity to 5-fluorouracil in mouse and human cells in culture. Cancer Res. 1979;39:383–90.
14. Tsume Y, Hilfinger JM, Amidon GL. Enhanced cancer cell growth inhibition by dipeptide prodrugs of floxuridine: increased transporter affinity and metabolic stability. Mol Pharm. 2008;5:717–27.
15. Burris 3rd HA, Moore MJ, Andersen J, Green MR, Rothenberg ML, Modiano MR, *et al.* Improvements in survival and clinical benefit with gemcitabine as first-line therapy for patients with advanced pancreas cancer: a randomized trial. J Clin Oncol. 1997;15:2403–13.
16. Barton-Burke M. Gemcitabine: a pharmacologic and clinical overview. Cancer Nurs. 1999;22:176–83.
17. Heinemann V, Hertel LW, Grindey GB, Plunkett W. Comparison of the cellular pharmacokinetics and toxicity of 2′,2′-difluorodeoxycytidine and 1-beta-D-arabinofuranosylcytosine. Cancer Res. 1988;48:4024–31.
18. Plunkett W, Huang P, Gandhi V. Preclinical characteristics of gemcitabine. Anticancer Drugs. 1995;6 Suppl 6:7–13.
19. Plunkett W, Huang P, Xu YZ, Heinemann V, Grunewald R, Gandhi V. Gemcitabine: metabolism, mechanisms of action, and self-potentiation. Semin Oncol. 1995;22:3–10.
20. Tsume Y, Vig BS, Sun J, Landowski CP, Hilfinger JM, Ramachandran C, *et al.* Enhanced absorption and growth inhibition with amino acid monoester prodrugs of floxuridine by targeting hPEPT1 transporters. Molecules. 2008;13:1441–54.
21. Landowski CP, Vig BS, Song X, Amidon GL. Targeted delivery to PEPT1-overexpressing cells: acidic, basic, and secondary floxuridine amino acid ester prodrugs. Mol Cancer Ther. 2005;4:659–67.
22. Song X, Lorenzi PL, Landowski CP, Vig BS, Hilfinger JM, Amidon GL. Amino acid ester prodrugs of the anticancer agent gemcitabine: synthesis, bioconversion, metabolic bioevasion, and hPEPT1-mediated transport. Mol Pharm. 2005;2:157–67.
23. Behrens I, Kamm W, Dantzig AH, Kissel T. Variation of peptide transporter (PepT1 and HPT1) expression in Caco-2 cells as a function of cell origin. J Pharm Sci. 2004;93:1743–54.
24. Geromichalos GD, Trafalis DT, Katsoulos GA, Papageorgiou A, Dalezis P, Triandafillidis EB, *et al.* Synergistic interaction between a mixed ligand copper (II) chelate complex and two anticancer agents in T47D human breast cancer cells *in vitro*. J BUON. 2006;11:469–76.
25. Ohbayashi M, Yasuda M, Kawakami I, Kohyama N, Kobayashi Y, Yamamoto T. Effect of interleukins response to ECM-induced acquisition of drug resistance in MCF-7 cells. Exp Oncol. 2008;30:276–82.
26. Padron JM, van der Wilt CL, Smid K, Smitskamp-Wilms E, Backus HH, Pizao PE, *et al.* The multilayered postconfluent cell culture as a model for drug screening. Crit Rev Oncol Hematol. 2000;36:141–57.
27. Rubas W, Jezyk N, Grass GM. Mechanism of dextran transport across rabbit intestinal tissue and a human colon cell-line (CACO-2). J Drug Target. 1995;3:15–21.
28. Zhao R, Raub TJ, Sawada GA, Kasper SC, Bacon JA, Bridges AS, *et al.* Breast cancer resistance protein interacts with various compounds *in vitro*, but plays a minor role in substrate efflux at the blood-brain barrier. Drug Metab Dispos. 2009;37:1251–8.
29. Au JL, Jang SH, Zheng J, Chen CT, Song S, Hu L, *et al.* Determinants of drug delivery and transport to solid tumors. J Control Release. 2001;74:31–46.

30. Minchinton AI, Tannock IF. Drug penetration in solid tumours. Nat Rev Cancer. 2006;6:583–92.
31. Rizvi I, Celli JP, Evans CL, Abu-Yousif AO, Muzikansky A, Pogue BW, *et al.* Synergistic enhancement of carboplatin efficacy with photodynamic therapy in a three-dimensional model for micrometastatic ovarian cancer. Cancer Res. 2010;70:9319–28.
32. Ohmori T, Yang JL, Price JO, Arteaga CL. Blockade of tumor cell transforming growth factor-betas enhances cell cycle progression and sensitizes human breast carcinoma cells to cytotoxic chemotherapy. Exp Cell Res. 1998;245:350–9.
33. Sharma SV, Haber DA, Settleman J. Cell line-based platforms to evaluate the therapeutic efficacy of candidate anticancer agents. Nat Rev Cancer. 2010;10:241–53.
34. del Carmen MG, Rizvi I, Chang Y, Moor AC, Oliva E, Sherwood M, *et al.* Synergism of epidermal growth factor receptor-targeted immunotherapy with photodynamic treatment of ovarian cancer *in vivo*. J Natl Cancer Inst. 2005;97:1516–24.
35. Molpus KL, Kato D, Hamblin MR, Lilge L, Bamberg M, Hasan T. Intraperitoneal photodynamic therapy of human epithelial ovarian carcinomatosis in a xenograft murine model. Cancer Res. 1996;56:1075–82.
36. Finlay JC, Mitra S, Patterson MS, Foster TH. Photobleaching kinetics of Photofrin *in vivo* and in multicell tumour spheroids indicate two simultaneous bleaching mechanisms. Phys Med Biol. 2004;49:4837–60.
37. Friedrich J, Ebner R, Kunz-Schughart LA. Experimental anti-tumor therapy in 3-D: spheroids—old hat or new challenge? Int J Radiat Biol. 2007;83:849–71.
38. Yamada KM, Cukierman E. Modeling tissue morphogenesis and cancer in 3D. Cell. 2007;130:601–10.
39. Horning JL, Sahoo SK, Vijayaraghavalu S, Dimitrijevic S, Vasir JK, Jain TK, *et al.* 3-D tumor model for *in vitro* evaluation of anticancer drugs. Mol Pharm. 2008;5:849–62.
40. Kunz-Schughart LA, Freyer JP, Hofstaedter F, Ebner R. The use of 3-D cultures for high-throughput screening: the multicellular spheroid model. J Biomol Screen. 2004;9:273–85.
41. Kim JB. Three-dimensional tissue culture models in cancer biology. Semin Cancer Biol. 2005;15:365–77.
42. Celli JP, Rizvi I, Evans CL, Abu-Yousif AO, Hasan T. Quantitative imaging reveals heterogeneous growth dynamics and treatment-dependent residual tumor distributions in a three-dimensional ovarian cancer model. J Biomed Opt. 2010;15:051603.
43. Debnath J, Brugge JS. Modelling glandular epithelial cancers in three-dimensional cultures. Nat Rev Cancer. 2005;5:675–88.
44. Monazzam A, Josephsson R, Blomqvist C, Carlsson J, Langstrom B, Bergstrom M. Application of the multicellular tumour spheroid model to screen PET tracers for analysis of early response of chemotherapy in breast cancer. Breast Cancer Res. 2007;9:R45.
45. Landowski CP, Song X, Lorenzi PL, Hilfinger JM, Amidon GL. Floxuridine amino acid ester prodrugs: enhancing Caco-2 permeability and resistance to glycosidic bond metabolism. Pharm Res. 2005;22:1510–8.
46. Vig BS, Lorenzi PJ, Mittal S, Landowski CP, Shin HC, Mosberg HI, *et al.* Amino acid ester prodrugs of floxuridine: synthesis and effects of structure, stereochemistry, and site of esterification on the rate of hydrolysis. Pharm Res. 2003;20:1381–8.
47. Beauchamp LM, Krenitsky TA. Acyclovir prodrugs: the road to valacyclovir. Drugs Future. 1993;18:619–28.
48. Beauchamp LM, Orr GF, De Miranda P, Burnette TC, Krenitsky TA. Amino acid ester prodrugs of acyclovir. Antiviral Chem Chemother. 1992;3:157–64.
49. Maag H. Ganciclovir pro-drugs: Synthesis and pre-clinical development of valganciclovir (Valcyte™)., *AAPS Annual Meeting*, Toronto, Canada., 2002.
50. Purifoy DJ, Beauchamp LM, de Miranda P, Ertl P, Lacey S, Roberts G, *et al.* Review of research leading to new anti-herpesvirus agents in clinical development: valaciclovir hydrochloride (256U, the L-valyl ester of acyclovir) and 882C, a specific agent for varicella zoster virus. J Med Virol. 1993;Suppl 1:139–45.
51. Jung D, Dorr A. Single-dose pharmacokinetics of valganciclovir in HIV- and CMV-seropositive subjects. J Clin Pharmacol. 1999;39:800–4.
52. Pescovitz MD, Rabkin J, Merion RM, Paya CV, Pirsch J, Freeman RB, *et al.* Valganciclovir results in improved oral absorption of ganciclovir in liver transplant recipients. Antimicrob Agents Chemother. 2000;44:2811–5.
53. Ganapathy ME, Huang W, Wang H, Ganapathy V, Leibach FH. Valacyclovir: a substrate for the intestinal and renal peptide transporters PEPT1 and PEPT2. Biochem Biophys Res Commun. 1998;246:470–5.
54. Han H, de Vrueh RL, Rhie JK, Covitz KM, Smith PL, Lee CP, *et al.* 5′-Amino acid esters of antiviral nucleosides, acyclovir, and AZT are absorbed by the intestinal PEPT1 peptide transporter. Pharm Res. 1998;15:1154–9.
55. Han HK, Oh DM, Amidon GL. Cellular uptake mechanism of amino acid ester prodrugs in Caco-2/hPEPT1 cells overexpressing a human peptide transporter. Pharm Res. 1998;15:1382–6.
56. Sugawara M, Huang W, Fei YJ, Leibach FH, Ganapathy V, Ganapathy ME. Transport of valganciclovir, a ganciclovir prodrug, via peptide transporters PEPT1 and PEPT2. J Pharm Sci. 2000;89:781–9.
57. Anand BS, Patel J, Mitra AK. Interactions of the dipeptide ester prodrugs of acyclovir with the intestinal oligopeptide transporter: competitive inhibition of glycylsarcosine transport in human intestinal cell line-Caco-2. J Pharmacol Exp Ther. 2003;304:781–91.
58. Eriksson AH, Elm PL, Begtrup M, Nielsen R, Steffansen B, Brodin B. hPEPT1 affinity and translocation of selected Gln-Sar and Glu-Sar dipeptide derivatives. Mol Pharm. 2005;2:242–9.
59. Friedrichsen GM, Chen W, Begtrup M, Lee CP, Smith PL, Borchardt RT. Synthesis of analogs of L-valacyclovir and determination of their substrate activity for the oligopeptide transporter in Caco-2 cells. Eur J Pharm Sci. 2002;16:1–13.
60. Meredith D, Temple CS, Guha N, Sword CJ, Boyd CA, Collier ID, *et al.* Modified amino acids and peptides as substrates for the intestinal peptide transporter PepT1. Eur J Biochem. 2000;267:3723–8.
61. Nielsen CU, Andersen R, Brodin B, Frokjaer S, Taub ME, Steffansen B. Dipeptide model prodrugs for the intestinal oligopeptide transporter. Affinity for and transport via hPepT1 in the human intestinal Caco-2 cell line. J Control Release. 2001;76:129–38.
62. Vabeno J, Lejon T, Nielsen CU, Steffansen B, Chen W, Ouyang H, *et al.* Phe-Gly dipeptidomimetics designed for the di-/tripeptide transporters PEPT1 and PEPT2: synthesis and biological investigations. J Med Chem. 2004;47:1060–9.
63. Lorenzi PL, Landowski CP, Song X, Borysko KZ, Breitenbach JM, Kim JS, *et al.* Amino acid ester prodrugs of 2-bromo-5,6-dichloro-1-(beta-D-ribofuranosyl)benzimidazole enhance metabolic stability *in vitro* and *in vivo*. J Pharmacol Exp Ther. 2005;314:883–90.
64. Song X, Vig BS, Lorenzi PL, Drach JC, Townsend LB, Amidon GL. Amino acid ester prodrugs of the antiviral agent 2-bromo-5,6-dichloro-1-(beta-D-ribofuranosyl)benzimidazole as potential substrates of hPEPT1 transporter. J Med Chem. 2005;48:1274–7.
65. Goolcharran C, Borchardt RT. Kinetics of diketopiperazine formation using model peptides. J Pharm Sci. 1998;87:283–8.
66. Larsen SW, Ankersen M, Larsen C. Kinetics of degradation and oil solubility of ester prodrugs of a model dipeptide (Gly-Phe). Eur J Pharm Sci. 2004;22:399–408.